

Supporting Information

Diversification of DIX domain-containing proteins in the SAR supergroup

Maria-Myrto Kostareli, Timo Westerink, Gabriel Couillaud, Maaria Peippo, Francine Govers, Dolf Weijers, Edouard Evangelisti

Supporting Files

Supporting File 1: Table of DIX and DIX-like domain-containing proteins used in this study.

Supporting File 2: Hidden Markov Model (HMM) used to identify DIX-like domains.

Supporting File 3: Protein spectra identified upon *Phytophthora palmivora* ATHOS pulldown.

Supporting Figures

Figure S1. Intrinsically disordered regions separate DIX-like and C-terminal domains in <i>Phytophthora palmivora</i> Musketeer proteins PORTHOS, ARAMIS, and DARTAGNAN	2
Figure S2. AlphaFold models of the C-terminal domains of PORTHOS, ARAMIS, and DARTAGNAN.	3
Figure S3. The intrinsically disordered regions of ATHOS and DARTAGNAN contain conserved short linear motifs (SLiMs)	4
Figure S4. Structural overlay of <i>Phytophthora palmivora</i> DIX-like domains and similar domains occurring in the SAR supergroup	5
Figure S5. Phylogenetic relationships of PORTHOS kinase domains with the kinome of <i>Phytophthora infestans</i>	6
Figure S6. AlphaFold model of the kinase domain of <i>Bremia lactucae</i> PORTHOS-like protein	7
Figure S7. Several oomycete PORTHOS-like proteins carry a DIX domain and short linear motifs reminiscent of ATHOS proteins	8
Figure S8. <i>Phytophthora palmivora</i> DIX-like domains are structurally similar to animal and plant DIX domains	9
Figure S9. Transcripts encoding the ATHOS protein accumulate in <i>Phytophthora palmivora</i> zoospores	10
Figure S10. Subcellular localization of <i>Phytophthora palmivora</i> ATHOS in zoospores and early cysts	11
Figure S11. Subcellular localization of <i>Phytophthora palmivora</i> Centrin 2 in zoospores	12

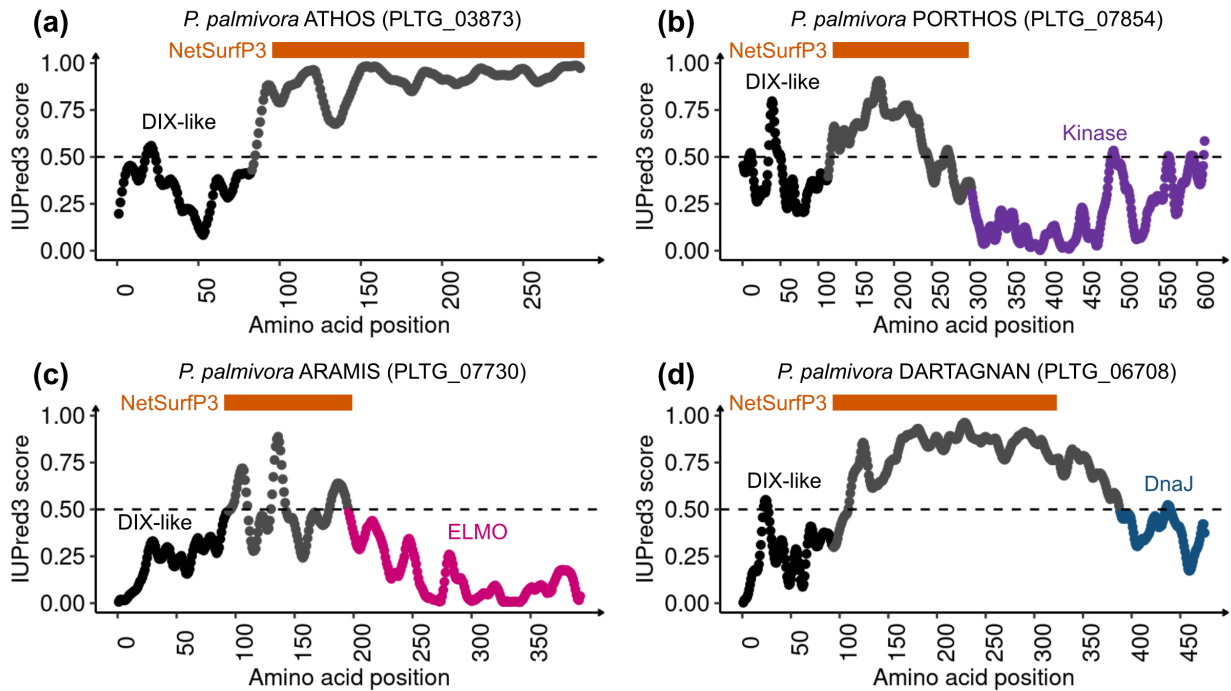


Figure S1. Intrinsically disordered regions separate DIX-like and C-terminal domains in *Phytophthora palmivora* Musketeer proteins PORTHOS, ARAMIS, and DARTAGNAN. (a-d) The amino acid sequences of *P. palmivora* Musketeer proteins ATHOS (PLTG_03873) (a), PORTHOS (PLTG_07854) (b), ARAMIS (PLTG_07730) (c), and DARTAGNAN (PLTG_06708) (d) were analyzed for intrinsically disordered regions using IUPred3 (Erdős *et al.*, 2021) and NetSurfP3 (Høie *et al.*, 2022). The graphs display IUPred3 scores along the sequences. DIX-like domains are highlighted in black, while C-terminal domains are indicated in purple (kinase), pink (ELMO), or blue (DnaJ). Qualitative predictions from NetSurfP3 are shown in orange.

References:

- Erdős G, Pajkos M, Dosztányi Z (2021). IUPred3: prediction of protein disorder enhanced with unambiguous experimental annotation and visualization of evolutionary conservation. *Nucleic Acids Research* 49 (W1): W297–W303.
- Høie MH, Kiehl EN, Petersen B, Nielsen M, Winther O, Nielsen H, Hallgren J, Marcatili P (2022). NetSurfP-3.0: accurate and fast prediction of protein structural features by protein language models and deep learning. *Nucleic Acids Research* 50 (W1): W510–W515.

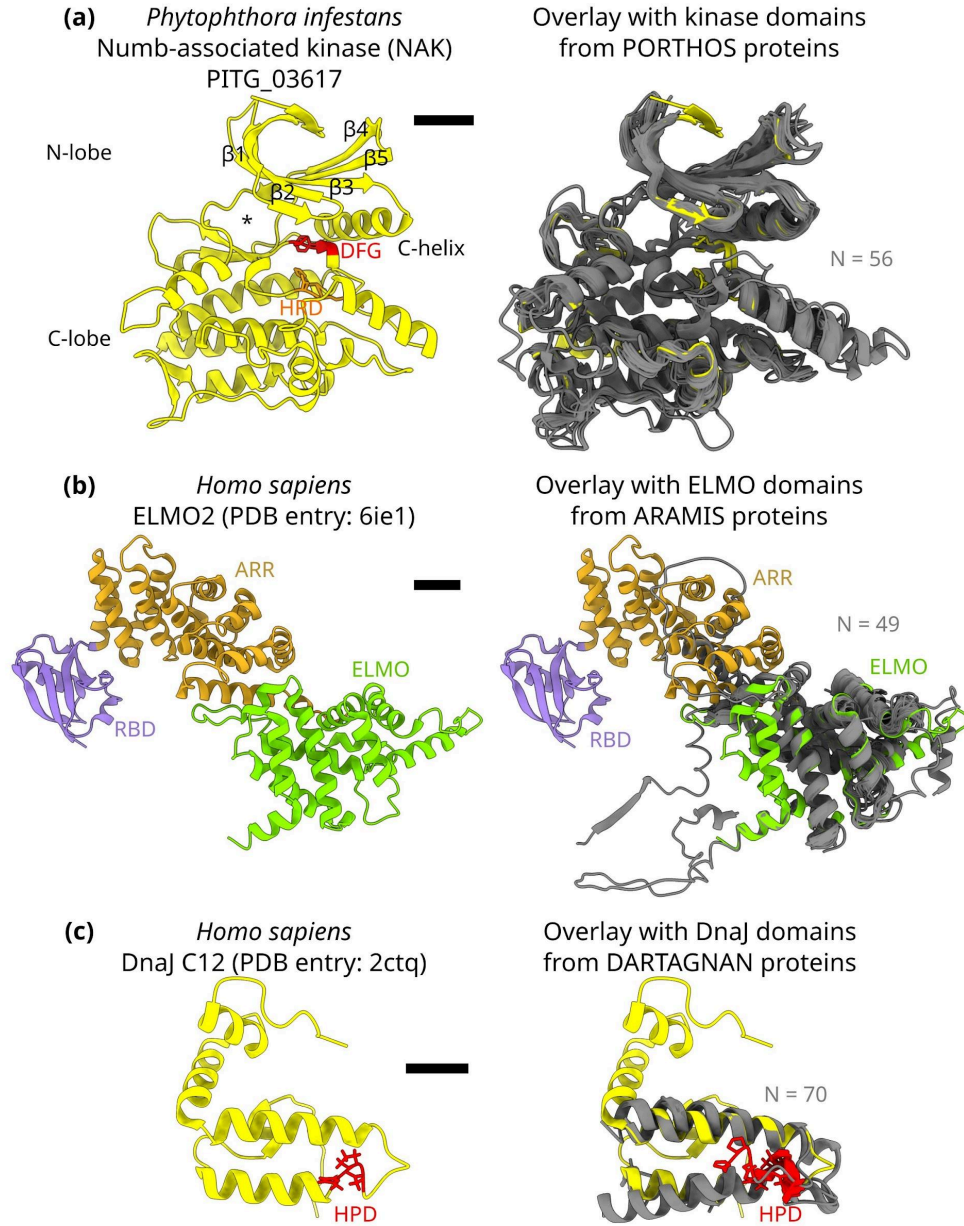


Figure S2. AlphaFold models of the C-terminal domains of PORTHOS, ARAMIS, and DARTAGNAN. (a) Numb-associated kinase (NAK)-like kinase domains of PORTHOS proteins (grey), overlaid with the AlphaFold model of *Phytophthora infestans* NAK (PITG_03617) (yellow). The conserved DFG and HRD motifs are highlighted in red and yellow, respectively. Asterisks indicate the ATP binding pocket. (b) Engulfment and cell motility (ELMO) domains of ARAMIS proteins (grey) compared to the crystal structure of *Homo sapiens* ELMO2 (PDB entry: 6ie1). The Ras-binding domain (RBD), armadillo repeats domain (ARR), and ELMO domain are shown in purple, orange, and green, respectively. (c) J domains of DARTAGNAN proteins (grey) overlaid with the J domain of *Homo sapiens* DnaJ C12 (PDB entry: 2ctq) (yellow). The DnaK-binding sequence HPD is shown in red. N indicates the number of overlaid domains. Scale bars: 1 nm.

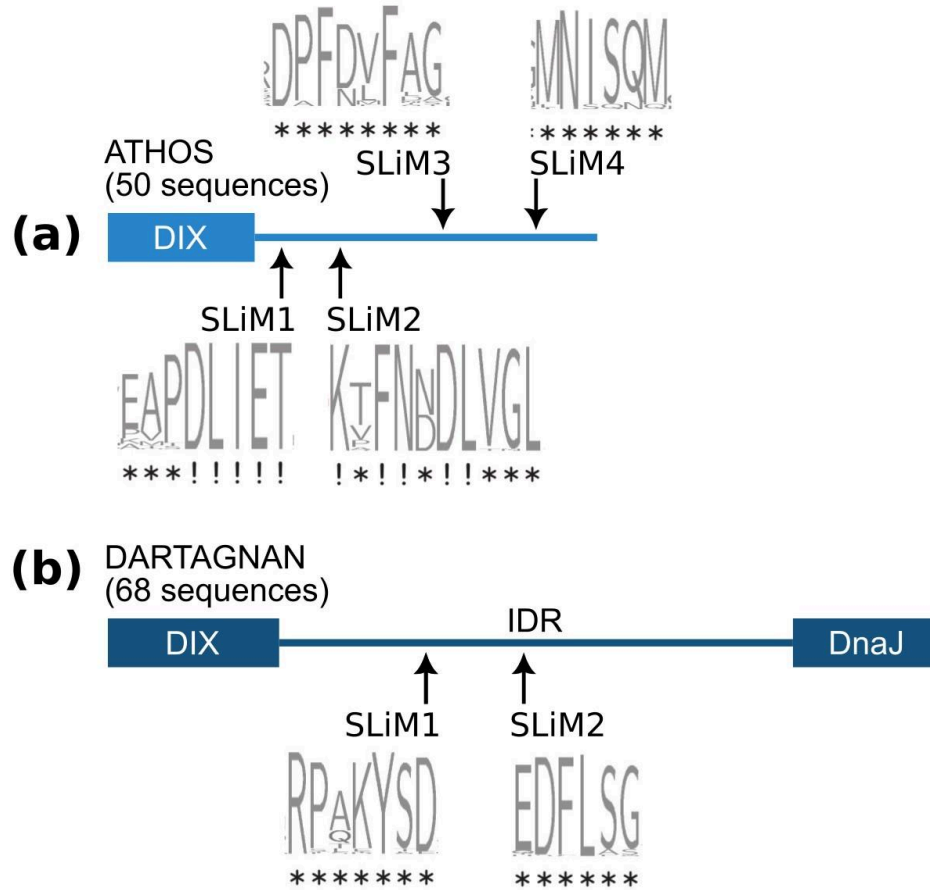


Figure S3. The intrinsically disordered regions of ATHOS and DARTAGNAN contain conserved short linear motifs (SLiMs). (a) ATHOS SLiMs were identified from a subset of 50 sequences from oomycete species. (b) DARTAGNAN SLiMs were identified from a subset of 68 sequences. In the sequence logos, letter size reflects the sequence conservation level.

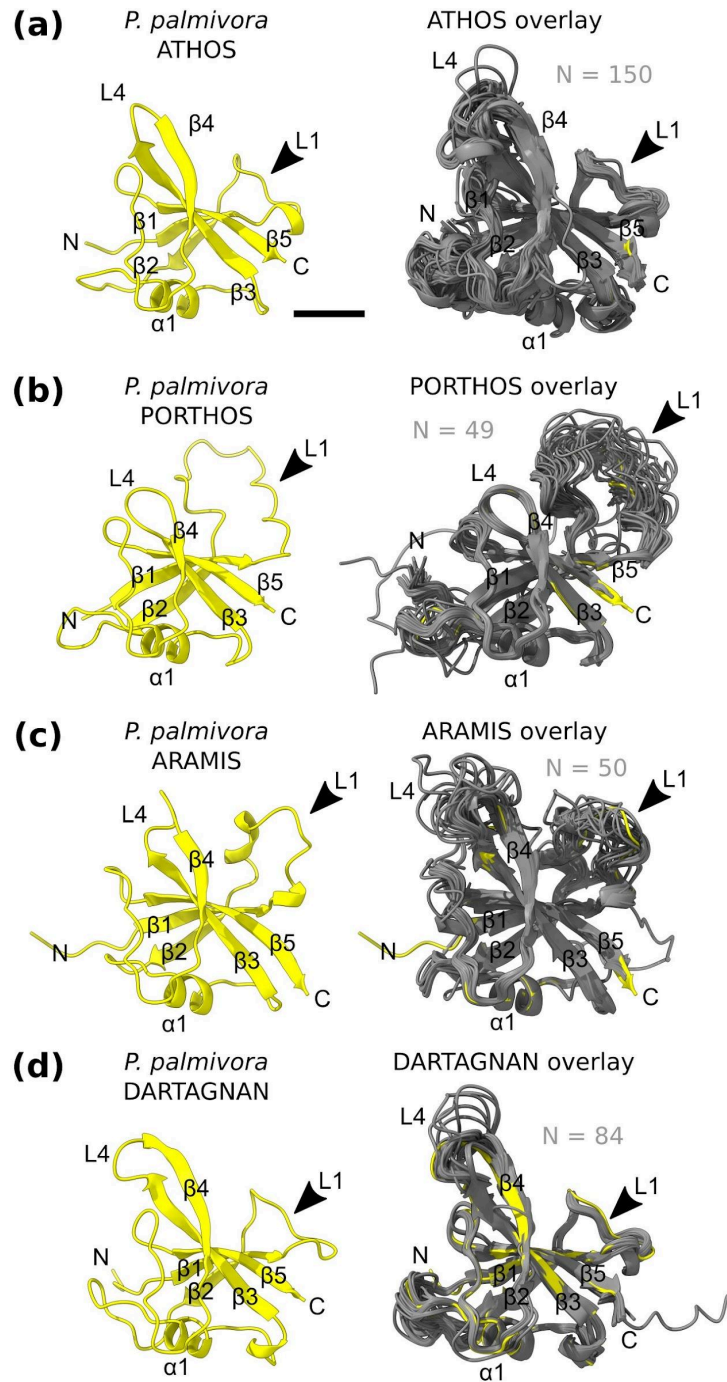


Figure S4. Structural overlay of *Phytophthora palmivora* DIX-like domains and similar domains occurring in the SAR supergroup. (a-d) AlphaFold models of DIX-like domains from the *P. palmivora* Musketeer proteins ATHOS (a), PORTHOS (b), ARAMIS (c), and DARTAGNAN (d) (yellow) were overlaid with DIX-like domains from similar proteins within the SAR supergroup (grey). N indicates the number of overlaid domains. Scale bar: 1 nm.

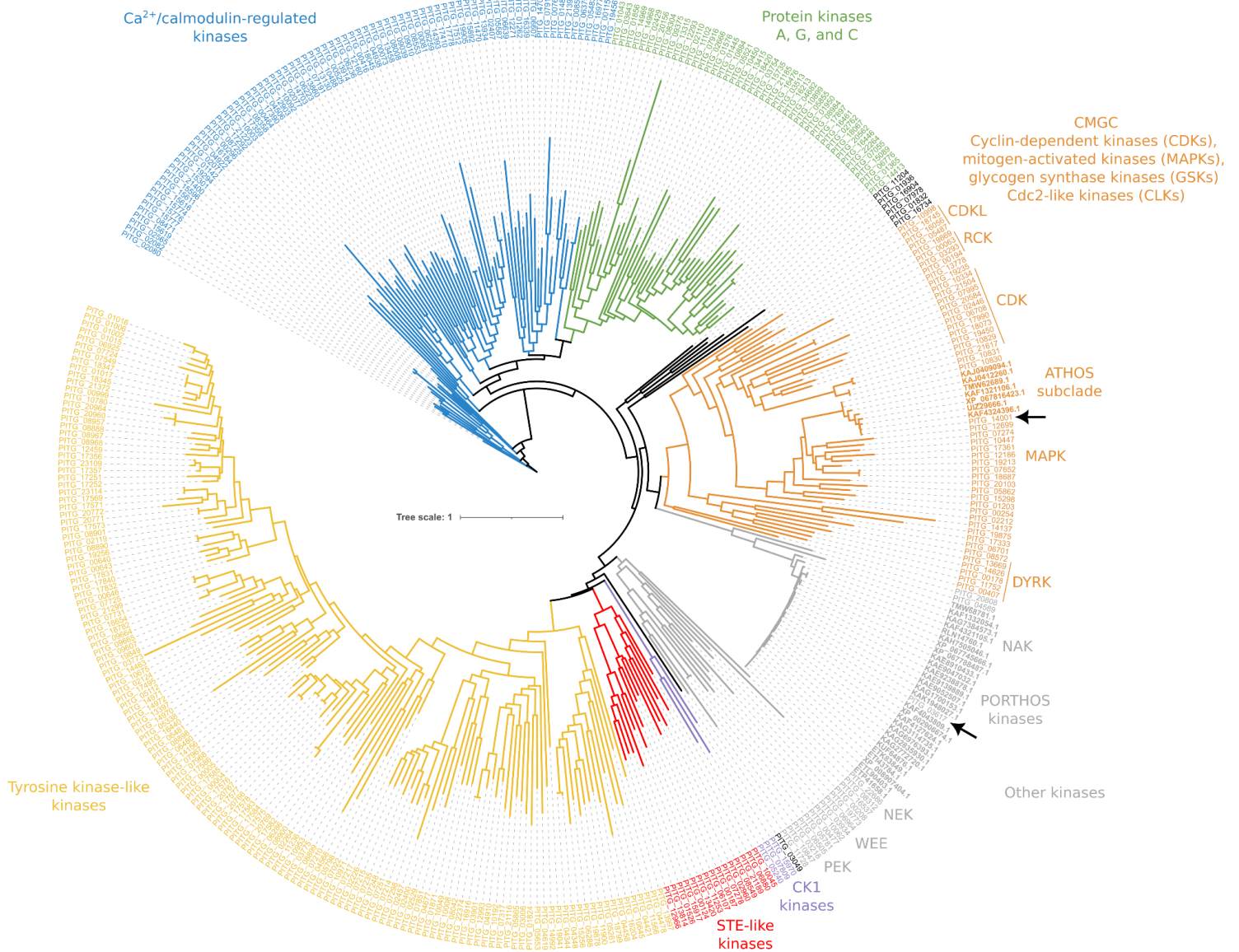


Figure S5. Phylogenetic relationships of PORTHOS kinase domains with the kinome of *Phytophthora infestans*. Illustrated is a maximum likelihood tree based on catalytic domains. Groups are highlighted and color-coded according to Judelson & Ah-Fong (2010). Arrows indicate the *P. infestans* kinases with the highest amino acid sequence similarity to PORTHOS kinases.

Reference:

Judelson HS, Ah-Fong AM (2010). The kinome of *Phytophthora infestans* reveals oomycete-specific innovations and links to other taxonomic groups. *BMC Genomics* 11: 700.

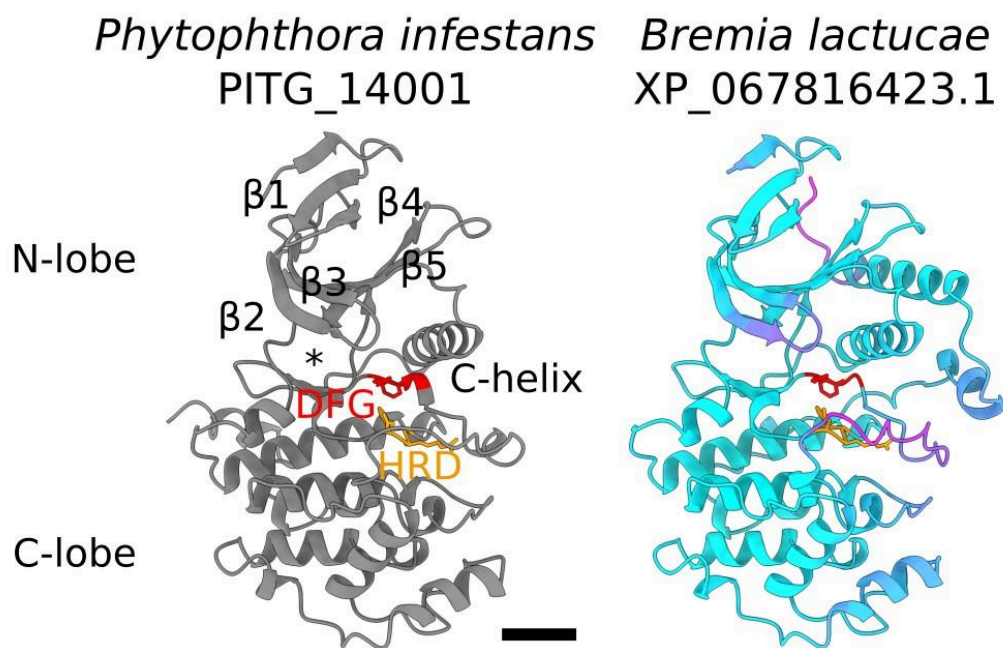


Figure S6. AlphaFold model of the kinase domain of *Bremia lactucae* PORTHOS-like protein. *B. lactucae* PORTHOS-like protein features a mitogen-activated protein kinase (MAPK)-type kinase domain with a functional catalytic site. The conserved DFG and HRD motifs are highlighted in red and yellow, respectively, while asterisks indicate the ATP binding pocket. Model confidence is represented by a color gradient transitioning from magenta (low confidence) to cyan (high confidence). Scale bar: 1 nm.

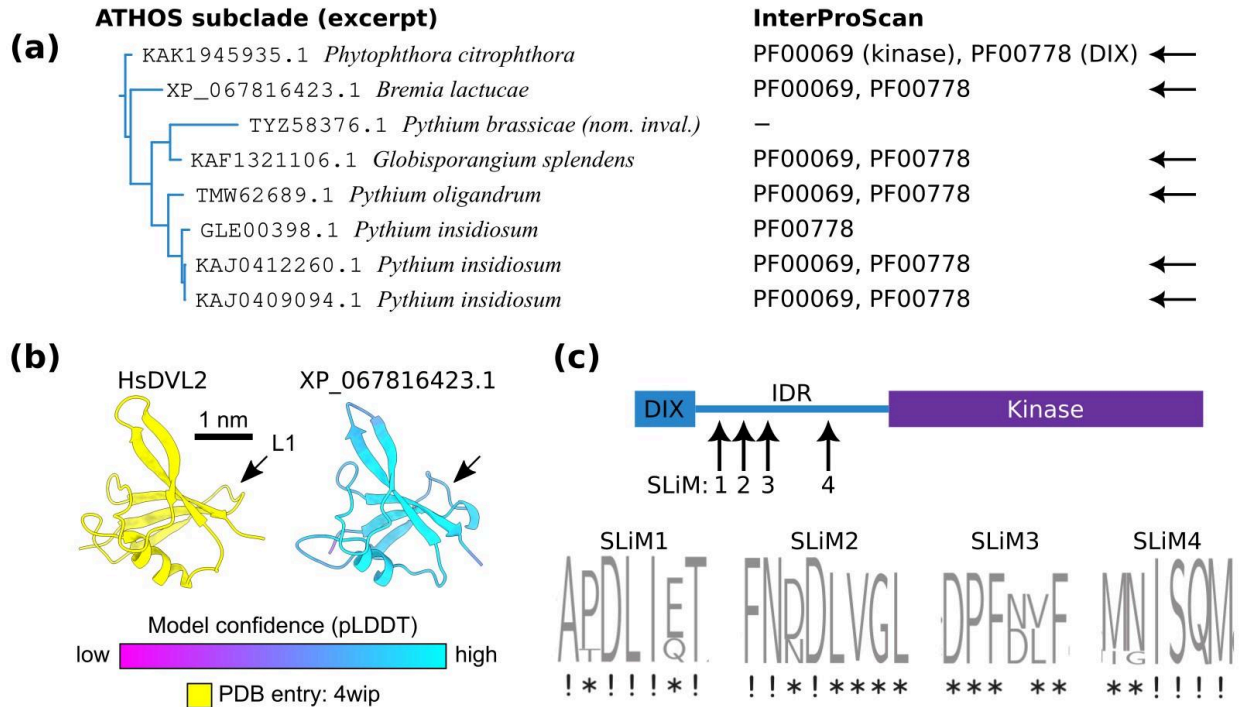


Figure S7. Several oomycete PORTHOS-like proteins carry a DIX domain and short linear motifs reminiscent of ATHOS proteins. (a) Detailed view of an ATHOS subclade containing PORTHOS-like proteins that possess DIX (PF00778) and protein kinase (PF00069) domains, indicated by arrows. (b) AlphaFold model of the DIX domain of *Bremia lactucae* protein XP_067816423.1. The crystal structure of *Homo sapiens* DISHEVELLED 2 (HsDVL2) DIX domain was used as a reference. Scale bar: 1 nm. (c) Short linear motifs (SLiMs) identified in the intrinsically disordered regions of PORTHOS-like proteins.

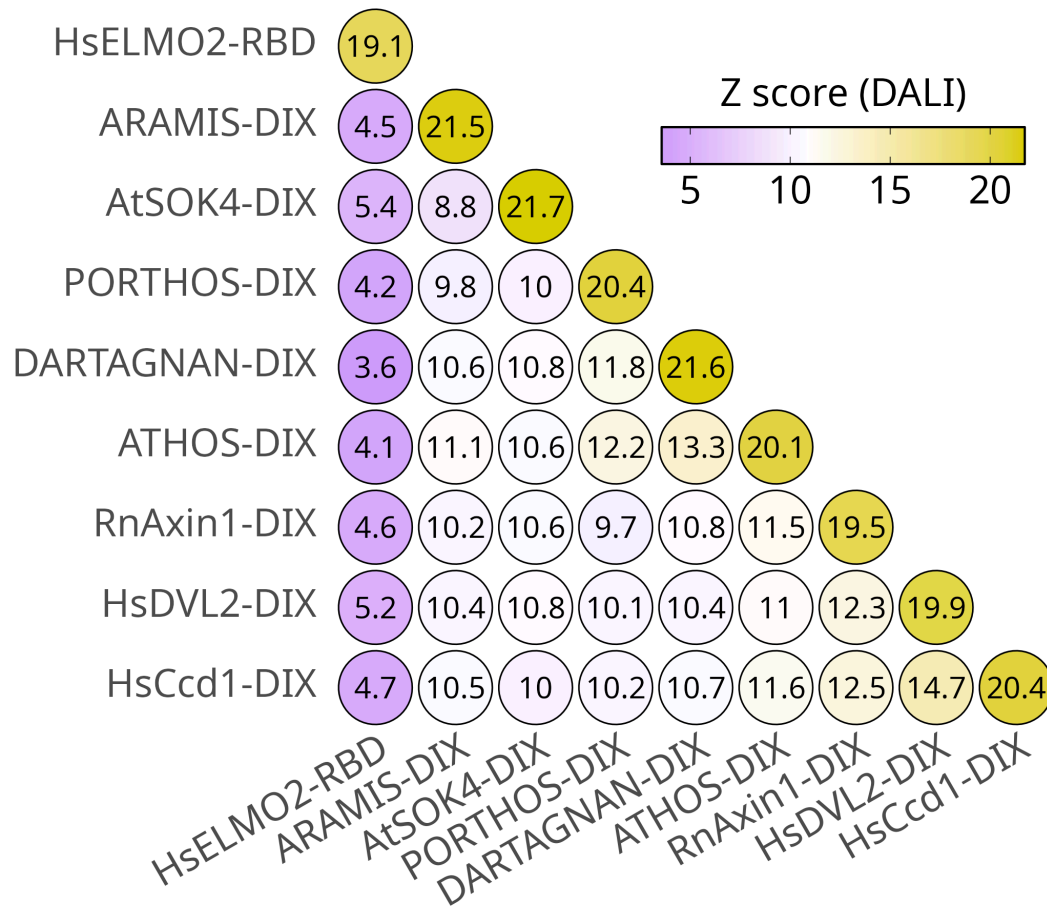


Figure S8. *Phytophthora palmivora* DIX-like domains are structurally similar to animal and plant DIX domains. AlphaFold models of DIX-like domains from the *P. palmivora* Musketeer proteins ATHOS, PORTHOS, ARAMIS, and DARTAGNAN were compared to those of *Homo sapiens* DVL2 (HsDVL2), DIXIN (HsCcd1), *Rattus norvegicus* Axin 1 (RnAxin1), and *Arabidopsis thaliana* SOK4 (AtSOK4) DIX domains using the DALI protein structure comparison server (Holm *et al.*, 2023). The Ras-binding domain (RBD) from *Homo sapiens* ELMO2 (HsELMO2) served as a control due to its ubiquitin-like fold. The numbers in the circles correspond to Z-scores, visually represented with a color gradient transitioning from purple (Z-score < 5) to yellow (Z-score > 15).

Reference:

Holm L, Laiho A, Törönen P, Salgado M (2023). DALI shines a light on remote homologs: One hundred discoveries. Protein Science 32(1):e4519.

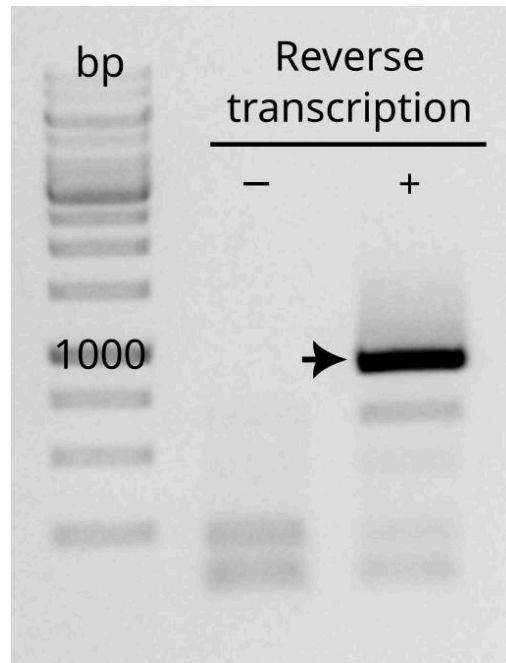


Figure S9. Transcripts encoding the ATHOS protein accumulate in *Phytophthora palmivora* zoospores. Total RNAs were extracted from *P. palmivora* zoospores and treated with DNase to remove DNA contamination. Purified RNAs were then used for reverse transcription using a blend of oligo(dT) and random hexamers (iScript cDNA Synthesis Kit, Bio-Rad). A reaction lacking reverse transcriptase (lane –) was used as negative control for RT-PCR. ATHOS was amplified using the forward primer ATHOS_F (5'-ATGGAGGGAATGCTCAACTACTACGTGC -3') and the reverse primer ATHOS_R (5'-CCATTGTCTCTGATTCGGGTTCTCT-3'). The amplicon (arrow) was validated by Sanger sequencing (Eurofins Genomics, Germany). bp: base pairs.

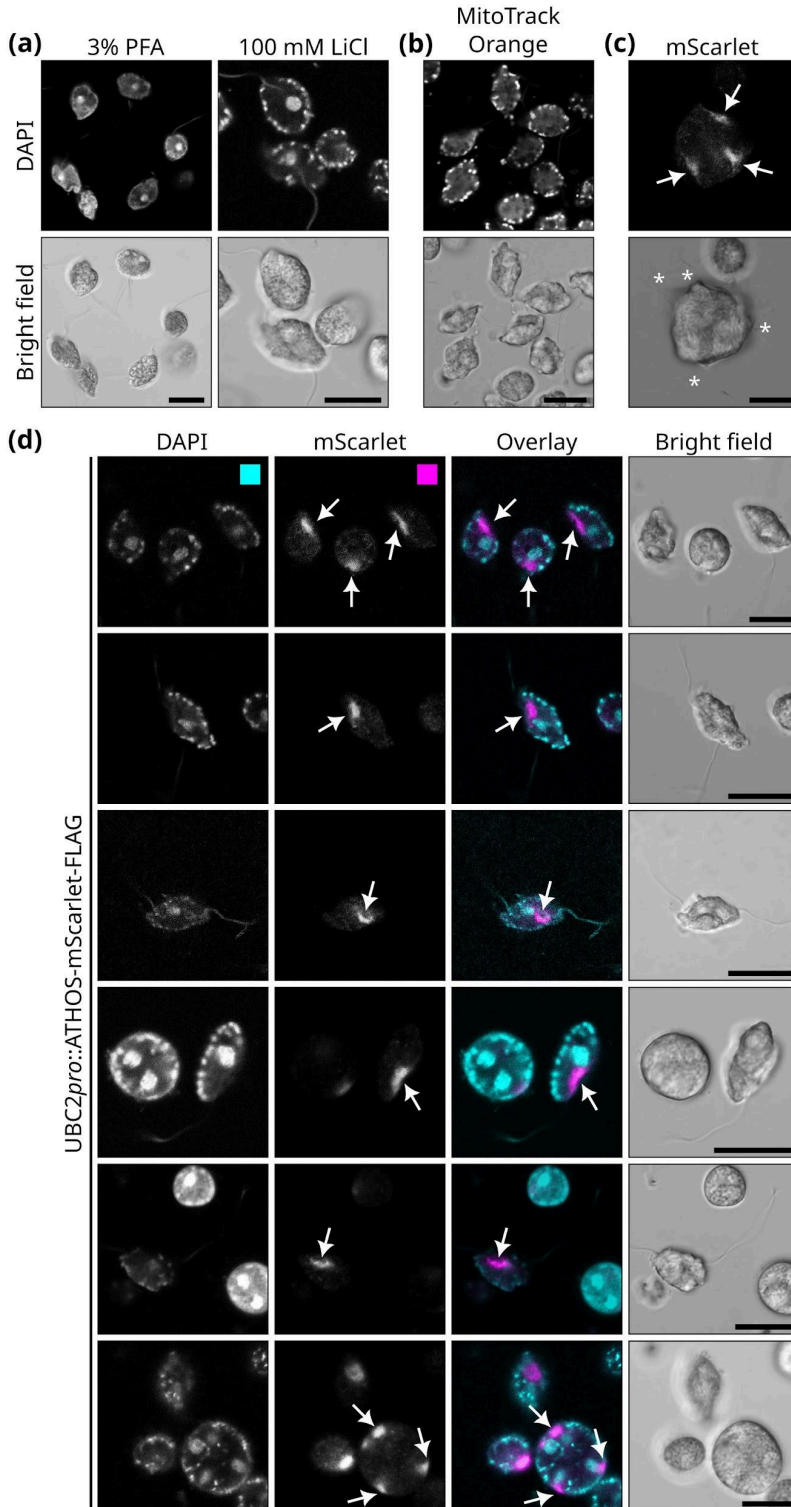


Figure S10. Subcellular localization of *Phytophthora palmivora* ATHOS in zoospores and early cysts. (a) Representative images of *P. palmivora* zoospores stained with DAPI after fixation with 3% paraformaldehyde (PFA, left) or non-lethal immobilization in the presence of 100 mM lithium chloride at 4°C (LiCl, right). (b) Representative images of *P. palmivora* zoospores stained with MitoTrack Orange CMTMRos after non-lethal immobilization in lithium chloride. (c) Abnormally shaped zoospore from a transgenic *P. palmivora* strain expressing the chimeric protein ATHOS-mScarlet under the control of the strong *UBC2* promoter. White arrows indicate ATHOS accumulations and white asterisks indicate flagella. (d) Subcellular localization of ATHOS in zoospores and early cysts. Zoospores were treated with lithium chloride and stained with DAPI before imaging. Arrows indicate ATHOS accumulations. Scale bars: 10 μ m.

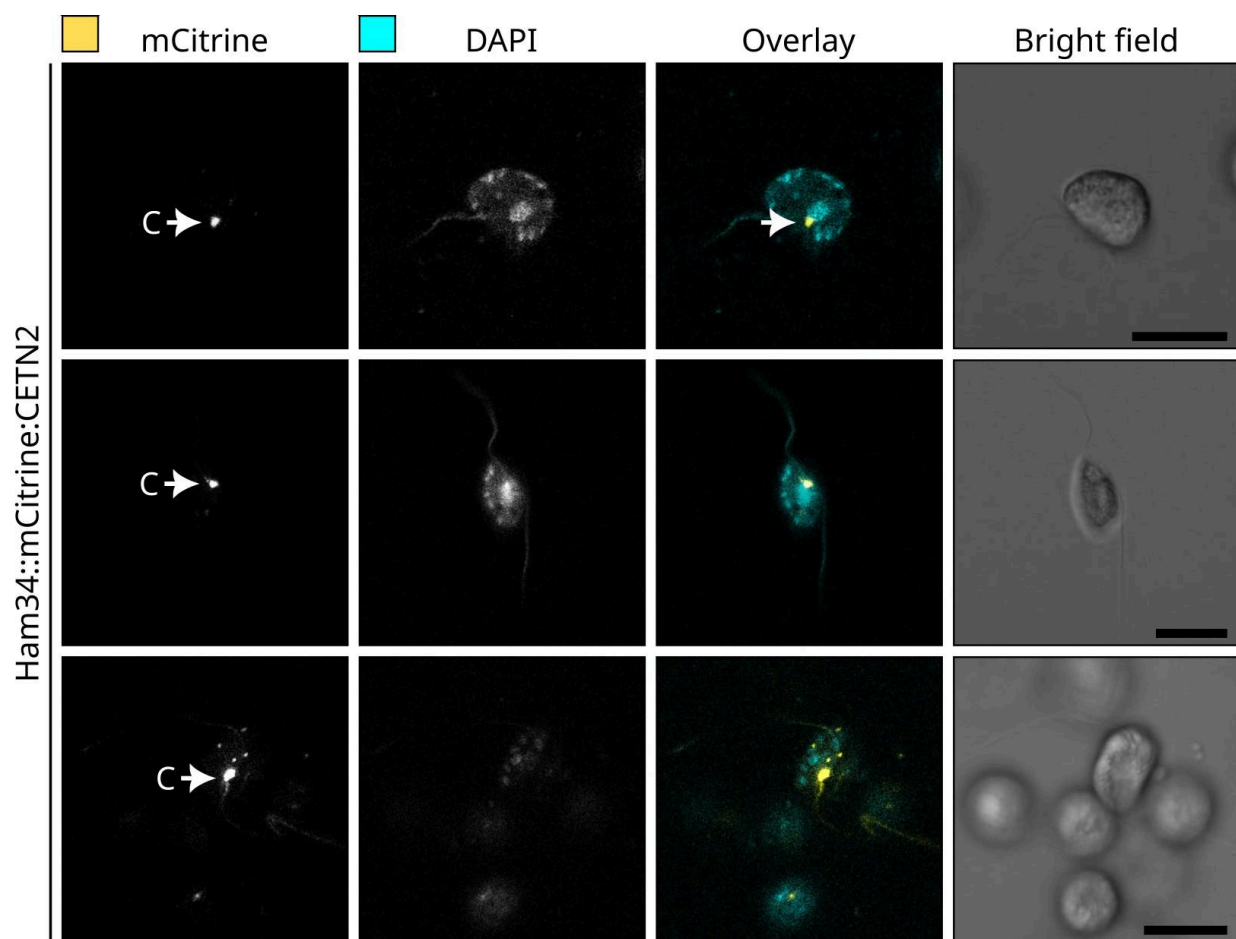


Figure S11. Subcellular localization of *Phytophthora palmivora* Centrin 2 in zoospores. Representative images of zoospores from a transgenic *P. palmivora* strain expressing a mCitrine-Centrin 2 fusion under the control of *Bremia lactucae* Ham34 promoter (Ham34::mCitrine-CETN2). Zoospores were treated with lithium chloride and stained with DAPI before imaging. C: centrosome. Scale bars: 10 μ m.